Pseudopaline, a staphylopine-like metallophore involved in zinc and nickel uptake in *Pseudomonas aeruginosa*

Sébastien Lhospice[1,§], Nicolas Oswaldo Gomez[1,§], Laurent Ouerdane[2,§], Catherine Brutesco[3], Ghassan Ghssein[3], Christine Hajjar[3], Ahmed Liratni[1], Shuanglong Wang[2], Pierre Richaud[4], Sophie Bleves[1], Geneviève Ball[1], Elise Borezée-Durant[5], Ryszard Lobinski[2], David Pignol[3], Pascal Arnoux[3,*] and Romé Voulhoux[1,*]

[1]CNRS et Aix-Marseille Université, Laboratoire d'Ingénierie des Systèmes Macromoléculaires (UMR7255), Institut de Microbiologie de la Méditerranée, Marseille, France.

[2]Université de Pau et des Pays de l'Adour/CNRS, Laboratoire de Chimie Analytique Bio-inorganique et Environnement, IPREM-UMR5254, Hélioparc, 2, Avenue Angot, 64053 Pau, France.

[3]CEA, CNRS and Aix-Marseille Université, Institut de Biosciences et Biotechnologies d'Aix-16 Marseille, UMR 7265 LBC, CEA Cadarache, Saint-Paul-lez-Durance F-13108, France.

[4]CEA, CNRS and Aix-Marseille Université, Institut de Biosciences et Biotechnologies d'Aix-Marseille, UMR 7265 LB3M, CEA Cadarache, Saint-Paul-lez Durance F-13108, France.

[5]Micalis Institute, INRA, AgroParisTech, Université Paris-Saclay, 78350 Jouy-en-Josas, France.

[§]Contributed equally to this work

[*]Correspondence E-mail: pascal.arnoux@cea.fr and voulhoux@imm.cnrs.fr

ABSTRACT

Metal uptake is vital for all living organisms. In metal scarce conditions, a common bacterial strategy consists in the biosynthesis of metallophores, their export in the extracellular medium and the recovery of a metal-metallophore complex through dedicated membrane transporters. Staphylopine is a recently described metallophore distantly related to plant nicotianamine that contributes to the broad-spectrum metal uptake capabilities of *Staphylococcus aureus*. Here, we characterize a four genes operon (*PA4837–PA4834*) in *Pseudomonas aeruginosa* involved in the biosynthesis and trafficking of a staphylopine-like metallophore named pseudopaline. Pseudopaline differs from staphylopine with regard to the stereochemistry of its histidine moiety associated to an alpha ketoglutarate moiety instead of pyruvate. *In vivo*, the pseudopaline operon is regulated by zinc through the Zur repressor. The metal-uptake property of the pseudopaline system appears different from that of staphylopine with a predominant effect on nickel uptake, and on zinc uptake in metal scarce conditions mimicking a chelating environment, thus reconciling the regulation of the *cnt* operon by zinc with its function as a zinc importer under metal scarce conditions.

AUTHOR SUMMARY

Zinc is an essential micronutrients for bacteria, particularly important at the host-pathogen interface where the host tends to sequester metals in a so called nutritional immunity framework, and the pathogenic bacterium increases its metal uptake efforts in order to keep up with its metal requirements. Here we reveal a novel metallophore, named pseudopaline, which is synthesized and exported by *Pseudomonas aeruginosa* and serves for the uptake of nickel in metal poor media, and for the uptake of zinc in metal scarce conditions that mimic the chelating environment that presumably prevails within a host.

53 **INTRODUCTION**

54 Divalent metals (Mn, Fe, Co, Ni, Cu and Zn) are essential micronutrients for all life forms,

55 and acquisition of these metals is therefore vital, particularly for bacterial pathogens in the

56 context of host-pathogen interactions. Indeed, there is a competition between the host, which

57 tends to sequester metals in a so called nutritional immunity framework, and the pathogenic

58 bacterium, which increases its metal uptake efforts in order to keep up with its metal

59 requirements (1, 2). Most pathogenic bacteria produce metallophores for metal uptake, with

60 siderophores being the most well-characterized metallophore family (3). Siderophores are

61 synthesized within the cell through non ribosomal peptide synthases (NRPS) or through a

62 NRPS independent system (NIS) and then are exported in the extracellular medium where

63 they scavenge iron. Extracellular iron siderophore complexes can be recognized and actively

64 transported into the periplasm by TonB dependent transporters (TBDT) in Gram-negative

65 bacteria, and usually ABC transporters in both Gram-negative and Gram-positive bacteria are

66 used for the crossing of the cytoplasmic membrane. There are many variations on this

67 common theme and, for example, some bacteria do not produce a specific type of siderophore

68 although they are able to use it for iron import (4). The siderophore pathway could also

69 prevent toxic accumulation of metals, which was particularly studied in the case of

70 *Pseudomonas aeruginosa* (5, 6). *P. aeruginosa* synthesizes two types of siderophores with

71 high iron affinity, pyochelin and pyoverdine, the latter being a demonstrated virulence factor

72 (7).

73 Metallophores specific for the uptake of metals other than iron have also been described, such

74 as the chalcophore methanobactin involved in copper uptake in methane-oxidizing bacteria (8,

75 9). Manganesophore have not been described as such, although TseM, a protein effector

76 secreted through a Type VI secretion system, was shown to play an important role in TBDT-

77 dependent manganese uptake in *Burkholderia thailandensis* (10). There is also indirect

78 evidence for the existence of a nickelophore in *Escherichia coli*, although it has still to be

79 identified (11). Free histidine could also be used as a nickelophore *in vivo* for nickel uptake in

80 various bacteria (12, 13). Yersiniabactin, initially described as a siderophore, also exhibits

81 zincophore properties in *Yersinia pestis* (14, 15). Coelibactin, described in *Streptomyces*

82 *coelicolor*, may also represent a zincophore as it is synthesized by a NRPS under the control

83 of Zur, a zinc responsive repressor (16).

84 Staphylopine is a nicotianamine-like molecule that was recently described as a metallophore

85 with remarkable broad-spectrum specificity (17). In *Staphylococcus aureus*, staphylopine is

86 synthesized through the action of three soluble enzymes (SaCntKLM). SaCntK transforms L-

87   histidine in D-histidine, SaCntL transfers an aminobutyrate moiety from S-
88   adenosylmethionine (SAM) onto D-histidine, and SaCntM reductively condensates the
89   product of SaCntL (called xNA) with pyruvate. The staphylopine biosynthesis and trafficking
90   pathway is responsible for zinc, copper, nickel, cobalt and iron uptake, depending on the
91   growth conditions, and this system contributes to the virulence and fitness of *S. aureus* (17–
92   19). The *S. aureus cnt* operon is partly conserved in *P. aeruginosa*, where homologues of the
93   *cntL* and *cntM* genes are found, albeit with 20-30% sequence identity at the protein level.
94   Upstream of *cntL*, a gene codes a predicted outer membrane protein belonging to the TBDT
95   family, and downstream of *cntM*, a gene codes for a predicted inner membrane protein
96   belonging to the EamA or DMT family (drug/metabolite transporter; Figure S1).
97   Transcriptomic approaches revealed that this gene cluster was highly expressed in a burn
98   wound model (20). This last gene was also identified as part of a novel siderophore pathway
99   that appeared vital for the growth of *P. aeruginosa* in airway mucus secretion (AMS) (21).
100   Finally, through a transcriptomic study of a Zur deficient strain, these four genes were found
101   in the top five regulated units, although most of them were annotated as hypothetical (22).
102   Here, we show that the four above-mentioned genes (here named *cntO*, *cntL*, *cntM* and *cntI;*
103   see supplementary table S1 for correspondence with locus tag in PAO1, PA7 and PA14
104   strains of *P. aeruginosa*) are part of an operon that is regulated by zinc level through the Zur
105   repressor. Using biochemistry and metabolomics approaches, we prove that the two
106   biosynthetic enzymes (PaCntL and PaCntM) synthesize a novel metallophore, which we
107   named pseudopaline, and which differs from staphylopine by the presence of a D-histidine
108   moiety instead of L-histidine, and an α-ketoglutarate moiety instead of a pyruvate. A *cntL*
109   mutant strain is shown to be unable to synthesize pseudopaline and is impaired in its ability to
110   import nickel in a minimal media, supplemented or not with nickel. Under more stringent
111   conditions where a chelator such as EDTA is added to a minimal succinate (MS) medium, a
112   condition that presumably mimics the chelating environment prevailing within a host or in
113   AMS, we show evidence that the *cntL* mutant strain is unable to import zinc, therefore
114   reconciling the regulation of this operon by zinc with its function as a zinc importer
115   functioning in metal scarce conditions.

116

117 **RESULTS AND DISCUSSION**

118 **The *cnt* operon of *P. aeruginosa* is regulated by zinc level through the zinc-responsive**

119 **regulator Zur**

120 *In silico* analysis of the *cnt* gene cluster of *P. aeruginosa* PA14 strain indicated two

121 overlapping open reading frames between *cntL* and *cntM* and between *cntM* and *cntI*,

122 classically observed in operonic structures (Figure S1). Further screening of the upstream *cnt*

123 sequence for promoter regions using Bprom software (23), revealed a σ70 promoter in the 200

124 base-pairs upstream from the annotated *cntO* ATG codon (Figure S1). Interestingly, a putative

125 Zur binding box "GTTATagtATAtC" can be identified overlapping the -10 box of the

126 predicted σ70 promoter, (22, 24). This *in silico* analysis supports an operonic organization of

127 the four *cnt* genes and strongly suggests a transcriptional activation of this operon under zinc

128 depletion through the Zur repressor (25, 26). In order to test this hypothesis, we performed

129 RT-PCR experiments using as templates RNA and cDNA generated from a WT PA14 strain

130 grown in minimal succinate (MS) medium known to contains low levels of metals, including

131 zinc (5). The successful amplification of the four *cnt* gene transcripts (Figure S1) indeed

132 indicated their induction when cells were grown in a MS medium. The specific amplification

133 of the three *cnt* intergenic regions confirmed that the four *cnt* genes are co-transcribed in one

134 single transcript and therefore constitute an operon.

135 To validate at the protein level the transcriptional regulation of the *cnt* genes, we followed by

136 immunoblotting the PaCntL production under various growth conditions. In this respect, we

137 constructed a *cntL* mutant strain producing a chromosomally encoded V5-tagged PaCntL

138 ($\Delta cntL::cntL_{V5}$). In this strain, the recombinant $cntL_{V5}$ gene was placed under the predicted *cnt*

139 promoter region and inserted at the *att* site of the *P. aeruginosa* genome. In agreement with

140 our transcriptional data, immunoblotting experiments indicated that, the recombinant

141 PaCntL$_{V5}$ is only produced in MS medium and not in a rich medium such as the LB medium

142 (Figure 1A). Presumably, this is due to the low metal content of the MS medium as compared

143 to the LB medium. We then tested whether the *cntL* transcription was subject to metal

144 repression by checking PaCntL$_{V5}$ production in MS medium supplemented with various

145 concentrations of the most representative metals. Dot-blot experiments showed a specific loss

146 of PaCntL$_{V5}$ production in MS medium supplemented with as low as 0.1 μM of ZnSO$_4$. An

147 addition of iron, nickel or cobalt at concentrations equivalent or above the one found in LB

148 rich medium (5) has no negative effect on PaCntL$_{V5}$ production (Figure 1B). The hypothesis

149 of a Zur repressor regulating the *cnt* operon was then tested through the construction of a

150 PA14$\Delta cntL::cntL_{V5}$ *zur*$^-$ strain. PaCntL$_{V5}$ was still produced in the *zur* mutant strain grown in

151 LB or MS media supplemented with 1 μM of $ZnSO_4$, conditions in which Zur normally exerts

152 its repressor activity (Figure 1C). Taken together, these data therefore demonstrate that the *cnt*

153 operon of *P. aeruginosa* is negatively regulated by zinc, most probably through the binding of

154 a Zn-Zur repressor complex onto the predicted Zur binding motif identified in the σ70

155 promoter, thus preventing the recruitment of RNA-polymerase.

156

In vivo detection and characterization of a PaCntL-dependent metallophore in the extracellular medium of *P. aeruginosa*

159 We constructed a PA14 mutant strain lacking PaCntL (Δ*cntL*) and compared the composition

160 of the intra- and extra-cellular contents of wild type and Δ*cntL* strains grown under the

161 previously defined *cnt* inducible conditions. Extracellular samples were analysed by

162 hydrophilic interaction liquid chromatography (HILIC) with detection by inductively coupled

163 plasma mass spectrometry (ICP-MS) and electrospray ionization mass spectrometry (ESI-

164 MS). HILIC/ICP-MS data revealed the presence of a molecule complexed with nickel and

165 zinc in the supernatant of the WT strain, which was absent in the *cntL* mutant strain (Figure

166 2). ESI-MS investigation of the metabolites eluting at this same elution volume showed

167 unambiguously the presence of typical nickel and zinc isotopic patterns indicating the

168 presence of a free metallophore with a molecular mass of 386 Da (Figure 2). Using the

169 accurate mass and a molecular formula finder software we proposed the $C_{15}N_4O_8H_{20}$ empiric

170 formula for the ligand in complex with nickel or zinc (Figure 2, inset for the nickel chelate).

171 This ligand corresponds to a new metallophore produced by *P. aeruginosa* in a *cntL*-

172 dependent manner. Comparison of its elemental composition with that of staphylopine (328

173 Da) revealed the presence of two additional carbons and two oxygen atoms, suggesting the

174 use of an α-ketoglutarate (αKG) moiety instead of pyruvate as found in staphylopine. The

175 fragmentation of this metallophore in gas-phase confirmed this hypothesis (Figure S2). We

176 propose to name this new metallophore pseudopaline, to recall its origin from *P. aeruginosa*

177 and its belonging to the nopaline family of opine (27).

178

In vitro reconstitution of the pseudopaline biosynthetic pathway catalysed by PaCntL and PaCntM

181 We have recently shown that the PaCntL/M orthologs in *S. aureus* (SaCntL/M) are

182 sequentially involved in the biosynthesis of the staphylopine metallophore, using a D-

183 histidine that is produced by the histidine racemase enzyme SaCntK (17). One of the main

184 difference between the *cnt* operons of *P. aeruginosa* and *S. aureus* is however the absence of

185   a *cntK* gene upstream of the *cntL-M* genes in *P. aeruginosa*. This observation led to the

186   possibility of using directly L-histidine instead of D-histidine. In order to investigate the

187   properties of CntL and CntM of *P. aeruginosa*, the corresponding genes were cloned,

188   heterologously expressed in *E. coli* and their products purified for further biochemical

189   analysis. Gel filtration experiments showed that PaCntL could form a complex with PaCntM

190   (Figure S3), although this interaction was not observed between SaCntL and SaCntM. With

191   regard to PaCntL, we used thin layer chromatography (TLC) separation to follow the carboxyl

192   moiety of a carboxyl-[^{14}C]-labelled S-adenosine methionine (SAM) substrate, co-incubated

193   with either L- or D-histidine (Figure 3A). Only the incubation with L-histidine led to a novel

194   band corresponding to a reaction intermediate that we propose to name yNA. We

195   demonstrated subsequently that PaCntM preferentially bound to NADH and not to NADPH

196   (Figure 3B), contrary to SaCntM that showed a preference for NADPH. We then used TLC to

197   visualize the PaCntLM reaction products under various *in vitro* conditions using all the

198   putative substrates (Figure 3C). Unexpectedly, the co-incubation of both enzymes with their

199   most probable substrates (L-histidine, NADH and αKG) did not lead to the formation of an

200   additional radiolabelled product as for the case of staphylopine biosynthesis (17) (Figure 3C).

201   One possibility was therefore that the product of PaCntM was migrating at the same position

202   as the yNA in the conditions used during the TLC separation. We therefore decided to study

203   the same co-incubations by HILIC/ESI-MS, following the mass expected for the yNA

204   intermediate and the pseudopaline found in the extracellular fraction of *P. aeruginosa* grown

205   in MS medium. These experiments confirmed that the incubation of PaCntL with SAM and

206   L-histidine led to the formation of the yNA reaction intermediate (Figure 3D, top), and most

207   of all, revealed the production of pseudopaline when co-incubating PaCntL, PaCntM and their

208   proposed substrates (SAM, L-histidine, NADH and αKG; Figure 3D, bottom). Co-incubations

209   using alternative substrates of PaCntM (pyruvate or NADPH) only led to the production of

210   yNA. Interestingly, pseudopaline and yNA eluted at the same volume in these HILIC-ESI/MS

211   experiments, showing that their physical properties are very similar, as suggested by our

212   previous TLC experiments.

213   Pseudopaline is therefore biosynthesized in two steps: first, a nucleophylic attack of one α-

214   aminobutyric acid moiety from SAM onto L-histidine catalysed by PaCntL to produce the

215   reaction intermediate yNA, and second, a NADH reductive condensation of the yNA

216   intermediate with a molecule of αKG catalysed by PaCntM to produce pseudopaline (Figure

217   3E). Pseudopaline differs from staphylopine by the stereochemistry of the histidine moiety

218   (L- and D- respectively) and by the presence of an αKG moiety instead of pyruvate in

219   staphylopine. The biosynthesis of a specific metallophore by different bacteria recalls the

220   chemical evolution of a large diversity of siderophore in a chemical rivalry to get access to

221   one's own pool of metal (28). Indeed, once in the extracellular medium, secreted

222   metallophores are a common good, and a privileged access presumably gives a selective

223   advantage.

224

225   **Pseudopaline is involved in nickel and zinc uptake, depending on the chelating**

226   **properties of the media**

227   In order to address the involvement of pseudopaline in metal uptake *in vivo*, we compared the

228   intracellular concentration of various metals in PA14 WT, *ΔcntL* and *ΔcntL::cntL* strains.

229   Cells were grown in pseudopaline-synthesis conditions determined above (MS medium) and

230   the intracellular metal concentration was measured by ICP-MS. Under these growth

231   conditions we observed a significant 90% reduction of intracellular nickel concentration in the

232   *ΔcntL* mutant strain (Figure 4A), which was mostly recovered in the complemented strain.

233   The levels of all the other metals were not changed in the *ΔcntL* mutant strain compared to the

234   WT strain (data not shown). A similar 90% reduction in intracellular nickel concentration was

235   also observed when the culture was supplemented with 1μM $NiCl_2$ (Figure S4), thus

236   confirming that nickel uptake was predominantly performed by pseudopaline in these metal-

237   poor media. We were intrigued by the apparent contradiction between the clear *cnt* operon

238   regulation by zinc, and the absence of any effect on zinc uptake. A possible explanation is that

239   the effect of *cnt* could be masked by the effect of a zinc ion importer such as the ZnuABC

240   zinc transport system described in *P. aeruginosa* (22). In an attempt to discriminate between

241   both transport systems, we sequestered free metal ions by supplementing the growth medium

242   with increasing concentrations of EDTA, a chelating agent for divalent metals. Interestingly,

243   although we did not observe any effect using 10 μM EDTA, the supplementation with 100μM

244   EDTA ultimately revealed a pseudopaline-dependent zinc uptake, with a 60% decrease of

245   intracellular zinc content in the *ΔcntL* mutant strain in comparison with the WT strain (Figure

246   4B). The complemented strain accumulated zinc to a level comparable to the WT. In these

247   chelating conditions the pseudopaline-dependent nickel import is abolished (Figure 4A),

248   hence proving a direct link between pseudopaline and zinc uptake in metal scarce conditions

249   with competing zinc chelators. These conditions may prevail at the host-pathogen interface

250   where metal binding proteins such as calprotectin are produced by the host (29, 30), or in

251   AMS where metals are complexed in a nutritional immunity framework (1, 21).

252

253 **Model of pseudopaline synthesis and transport pathway in *P. aeruginosa***

254 We next investigated the putative roles of the two membrane proteins that are found in the *cnt*

255 operon of *P. aeruginosa* by determining the pseudopaline level in the extracellular and

256 intracellular fractions of WT and mutant strains (Figure 5A and 5B, respectively). With

257 regard to PaCntO, we found a small decrease in the extracellular content of pseudopaline in

258 the Δ*cntO* mutant strain in comparison with the WT strain. However, we also found that this

259 Δ*cntO* mutant strain was partly impaired in nickel accumulation (Figure S5). Altogether, and

260 because PaCntO belongs to the TBDT family of extracellular transporter, its most probable

261 role is in the import of pseudopaline-metal complexes, although it is not excluded that other

262 proteins of this family could participate in this process. Next, we noted a large decrease in the

263 extracellular pseudopaline level in the Δ*cntI* mutant strain in comparison with the WT strain,

264 with a concomitant increase in the intracellular space, consistent with a role of PaCntI in

265 pseudopaline export. It is also interesting to note that a Δ*cntI* mutant strain is virtually unable

266 to grow in AMS (21). The most probable scenario is that this mutant is deficient in metal

267 content, including zinc, but pseudopaline accumulation in the cytoplasmic space actually

268 worsens the situation by chelating an already poorly available metal. This assumption is

269 supported by our finding that a double Δ*cntL*Δ*cntI* mutant supresses the detrimental growth

270 defect of the single Δ*cntI* mutant strain, *ie* the absence of pseudopaline restores the normal

271 growth of a mutant devoid of the pseudopaline exporter (Figure S6). A model recapitulating

272 the pseudopaline pathway is shown in Figure 5.

273 It is interesting to note the differences and similarities between staphylopine and pseudopaline

274 and between their respective biosynthetic pathways (Figure S7). On one hand, pseudopaline

275 differs from staphylopine by the incorporation of a L-histidine instead of a D-histidine moiety

276 in staphylopine, thus explaining the absence of amino acid racemase in *P. aeruginosa*.

277 Another particularity of pseudopaline is the use of an αKG moiety instead of pyruvate as

278 substrate for the second reaction mediated by PaCntM. Together this leads to two species-

279 specific metallophores that might give a selective advantage in a competing environment. The

280 fact that staphylopine and pseudopaline belong to Gram-positive and Gram-negative bacteria

281 has important consequences on their respective transport mechanisms across the two types of

282 bacterial envelopes. Although the transporters of staphylopine are well identified, the outer

283 membrane exporter pseudopaline and inner membrane importer of the pseudopaline-metal

284 complex remains to be discovered (Figure 5). Recycling of the metallophore could also take

285 place in *P. aeruginosa*, as recently exemplified in the case for pyoverdine (31). An interesting

286 aspect of this work is the discovery of two different pathways for the export of these

287 nicotianamine-like bacterial metallophores. Whereas *S. aureus* uses a protein belonging to the

288 MFS family (SaCntE) for staphylopine export, *P. aeruginosa* uses a protein belonging to the

289 DMT family of transporters, with PaCntI possessing two predicted EamA domains for

290 pseudopaline export. In the view of their importance in the growth or virulence of these

291 important human pathogens (19, 21), they could emerge as attractive targets for novel

292 antibiotic development.

293

ACKNOWLEDGEMENTS

300

REFERENCES

302 1.   Hood MI, Skaar EP (2012) Nutritional immunity: transition metals at the pathogen–

303 host interface. *Nat Rev Microbiol* 10(8):525–537.

304 2.   Weinberg ED (1975) Nutritional Immunity: Host's Attempt to Withhold Iron From

305 Microbial Invaders. *JAMA* 231(1):39–41.

306 3.   Budzikiewicz AG (2010) Siderophores from bacteria and from fungi. *Iron Uptake and

307 Homeostasis in Microorganisms* (Cornelis, P. and Andrews, S. C.), pp 1–16. Caister

308 Academic Press.

309 4.   Cornelissen CN, Hollander A (2011) TonB-Dependent Transporters Expressed by

310 Neisseria gonorrhoeae. *Front Microbiol* 2:117.

311 5.   Cunrath O, Geoffroy VA, Schalk IJ (2016) Metallome of *Pseudomonas aeruginosa*: a

312 role for siderophores. *Environ Microbiol* 18(10):3258–3267.

313 6.   Schalk IJ, Hannauer M, Braud A (2011) New roles for bacterial siderophores in metal

314 transport and tolerance. *Environ Microbiol* 13(11):2844–2854.

315 7.   Minandri F, et al. (2016) Role of Iron Uptake Systems in *Pseudomonas aeruginosa*

316 Virulence and Airway Infection. *Infect Immun* 84(8):2324–2335.

317 8.   Kim HJ, et al. (2004) Methanobactin, a copper-acquisition compound from methane-

318 oxidizing bacteria. *Science* 305(5690):1612–1615.

319 9.   Dassama LMK, Kenney GE, Ro SY, Zielazinski EL, Rosenzweig AC (2016)

320   Methanobactin transport machinery. *Proc Natl Acad Sci U S A* 113(46):13027–13032.

321   10.   Si M, et al. (2017) Manganese scavenging and oxidative stress response mediated by

322   type VI secretion system in *Burkholderia thailandensis*. *Proc Natl Acad Sci U S A*

323   114(11):E2233–E2242.

324   11.   Cherrier MV, Cavazza C, Bochot C, Lemaire D, Fontecilla-Camps JC (2008)

325   Structural characterization of a putative endogenous metal chelator in the periplasmic nickel

326   transporter NikA. *Biochemistry (Mosc)* 47(38):9937–9943.

327   12.   Lebrette H, et al. (2015) Novel insights into nickel import in *Staphylococcus aureus*:

328   the positive role of free histidine and structural characterization of a new thiazolidine-type

329   nickel chelator. *Metallomics*. doi:10.1039/C4MT00295D.

330   13.   Shaik MM, Cendron L, Salamina M, Ruzzene M, Zanotti G (2014) *Helicobacter*

331   *pylori* periplasmic receptor CeuE (HP1561) modulates its nickel affinity via organic

332   metallophores. *Mol Microbiol* 91(4):724–735.

333   14.   Bobrov AG, et al. (2014) The Yersinia pestis Siderophore, Yersiniabactin, and the

334   ZnuABC system both contribute to Zinc acquisition and the development of lethal septicemic

335   plague in mice. *Mol Microbiol*. doi:10.1111/mmi.12693.

336   15.   Bobrov AG, et al. (2017) Zinc transporters YbtX and ZnuABC are required for the

337   virulence of *Yersinia pestis* in bubonic and pneumonic plague in mice. *Met Integr Biometal*

338   *Sci* 9(6):757–772.

339   16.   Kallifidas D, et al. (2010) The zinc-responsive regulator Zur controls expression of the

340   coelibactin gene cluster in *Streptomyces coelicolor*. *J Bacteriol* 192(2):608–611.

341   17.   Ghssein G, et al. (2016) Biosynthesis of a broad-spectrum nicotianamine-like

342   metallophore in *Staphylococcus aureus*. *Science* 352(6289):1105–1109.

343   18.   Remy L, et al. (2013) The *Staphylococcus aureus* Opp1 ABC transporter imports

344   nickel and cobalt in zinc-depleted conditions and contributes to virulence. *Mol Microbiol*

345   87(4):730–743.

346   19.   Ding Y, Fu Y, Lee JC, Hooper DC (2012) *Staphylococcus aureus* NorD, a Putative

347   Efflux Pump Coregulated with the Opp1 Oligopeptide Permease, Contributes Selectively to

348   Fitness In Vivo. *J Bacteriol* 194(23):6586–6593.

349   20.   Bielecki P, et al. (2011) In-vivo expression profiling of *Pseudomonas aeruginosa*

350   infections reveals niche-specific and strain-independent transcriptional programs. *PloS One*

351   6(9):e24235.

352   21.   Gi M, et al. (2015) A novel siderophore system is essential for the growth of

353   *Pseudomonas aeruginosa* in airway mucus. *Sci Rep* 5:14644.

354   22.   Pederick VG, et al. (2015) ZnuA and zinc homeostasis in Pseudomonas aeruginosa.
355   *Sci Rep* 5:13139.

356   23.   Solovyev, V, Salamov A (2011) Automatic Annotation of Microbial Genomes and
357   Metagenomic Sequences. *Metagenomics and Its Applications in Agriculture, Biomedicine and*
358   *Environmental Studies* (Li, R.W.), pp 61–78. Nova Science Publishers.

359   24.   Pawlik M-C, et al. (2012) The zinc-responsive regulon of *Neisseria meningitidis*
360   comprises 17 genes under control of a Zur element. *J Bacteriol* 194(23):6594–6603.

361   25.   Patzer SI, Hantke K (2000) The zinc-responsive regulator Zur and its control of the
362   znu gene cluster encoding the ZnuABC zinc uptake system in *Escherichia coli*. *J Biol Chem*
363   275(32):24321–24332.

364   26.   Ellison ML, et al. (2013) The transcriptional regulator Np20 is the zinc uptake
365   regulator in *Pseudomonas aeruginosa*. *PloS One* 8(9):e75389.

366   27.   Thompson J, Donkersloot JA (1992) N-(carboxyalkyl)amino acids: occurrence,
367   synthesis, and functions. *Annu Rev Biochem* 61:517–557.

368   28.   Barber MF, Elde NC (2015) Buried treasure: evolutionary perspectives on microbial
369   iron piracy. *Trends Genet TIG* 31(11):627–636.

370   29.   Nakashige TG, et al. (2016) The Hexahistidine Motif of Host-Defense Protein Human
371   Calprotectin Contributes to Zinc Withholding and Its Functional Versatility. *J Am Chem Soc*
372   138(37):12243–12251.

373   30.   Subramanian Vignesh K, Deepe GS (2016) Immunological orchestration of zinc
374   homeostasis: The battle between host mechanisms and pathogen defenses. *Arch Biochem*
375   *Biophys* 611:66–78.

376   31.   Ganne G, et al. (2017) Iron Release from the Siderophore Pyoverdine in *Pseudomonas*
377   *aeruginosa* Involves Three New Actors: FpvC, FpvG, and FpvH. *ACS Chem Biol*
378   12(4):1056–1065.

379

380

381
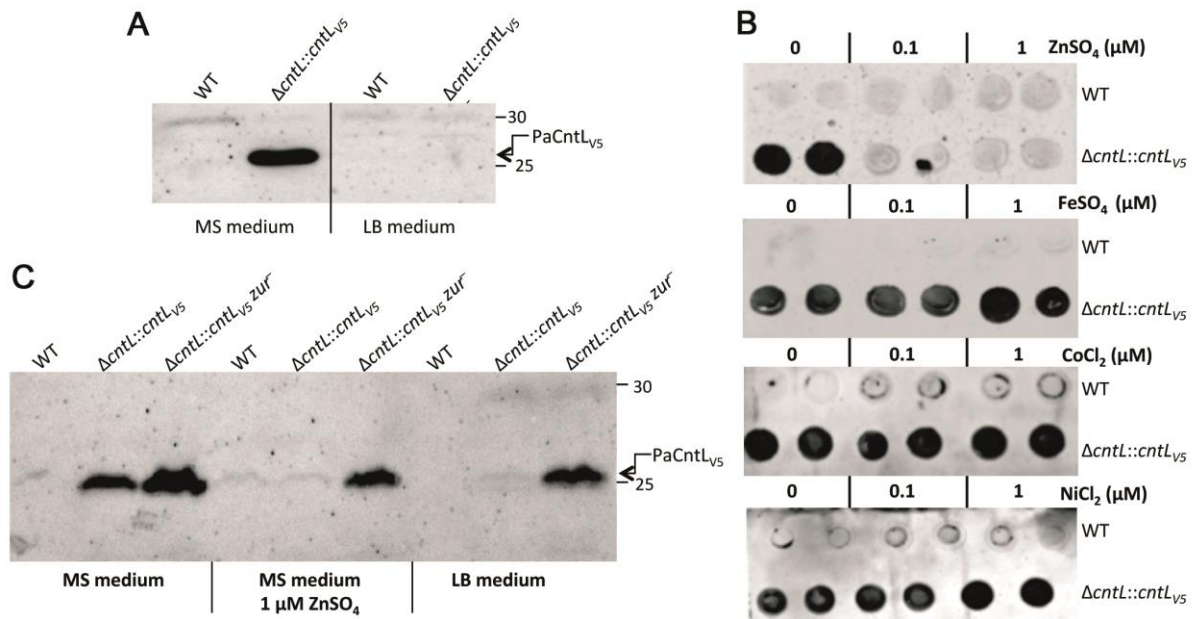
383

384 Figure 1: PaCntL production under various growth conditions. (A) Immunoblotting using
385 antibody directed against the V5 epitope for revealing PaCntL$_{V5}$ production under poor (MS)
386 and rich (LB) media. (B) Dot-blot revealing the Pa-CntL$_{V5}$ production in MS medium
387 supplemented by divalent metals. (C) Immunoblot detection of PaCntL$_{V5}$ production in PA14
388 WT and Zur deficient strains (*zur*⁻) in various growth conditions.

389

390
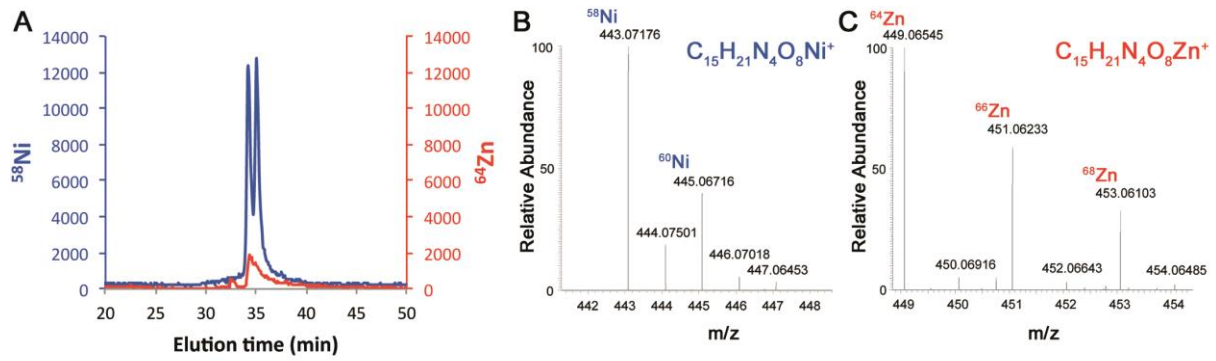
391

392 Figure 2: *In vivo* PaCntL-dependent detection of a nickel or zinc-bound metallophore in the

393 extracellular fraction of *P. aeuginosa*. (A) HILIC/ICP-MS chromatogram of metal-bound

394 metabolites. (B) HILIC-ESI/MS mass spectrum of a Ni-metallophore complex in the

395 extracellular fraction of the WT strain but absent in the Δ*cntL* mutant. (C) HILIC-ESI/MS

396 mass spectrum of a Zn-metallophore complex in the extracellular fraction of the WT strain but

397 absent in the Δ*cntL* mutant. The empirical molecular formula of the CntL-dependant Ni- or

398 Zn-metallophore complexes were deduced from the exact masse.

399
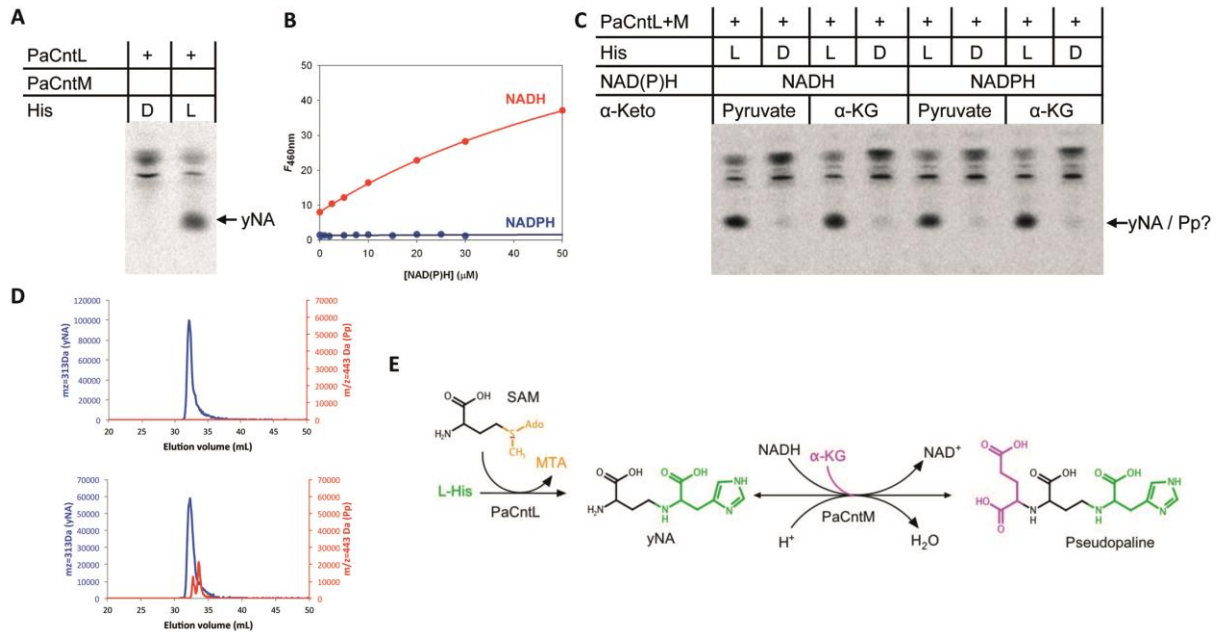
400
401 Figure 3: *In vitro* reconstitution of the pseudopaline biosynthesis pathway. (A) TLC
402 experiment using PaCntL and [^{14}C]-SAM showing that PaCntL discriminates between D- and
403 L-histidine substrate with the production of the reaction intermediate (noted yNA) only
404 visible when using L-histidine. (B) Titration of NADPH (blue) and NADH (red) binding to
405 PaCntM (5µM) followed by fluorescence resonance energy transfer. Fitting of the data
406 obtained for NADH led to a K_d of 30µM. (C) TLC separation of reaction products incubating
407 [^{14}C]-SAM using purified enzymes (PaCntL and PaCntM), different source of α-ketoacid
408 (pyruvate or α-KG), cofactor (NADH or NADPH) and histidine (L-His or D-His). (D)
409 HILIC/ESI-MS chromatograms of putative reaction products using PaCntL incubated with L-
410 histidine, revealing the production of the yNA intermediate (top), and a mix of PaCntL and
411 PaCntM incubated with all their putative substrate (SAM, L-histidine, NADH and α-
412 Ketaoglutarate), revealing the specific detection of pseudopaline in this case (red trace,
413 bottom). (E) Summary of the PaCntL/M-dependent biosynthesis pathway for the assembly of
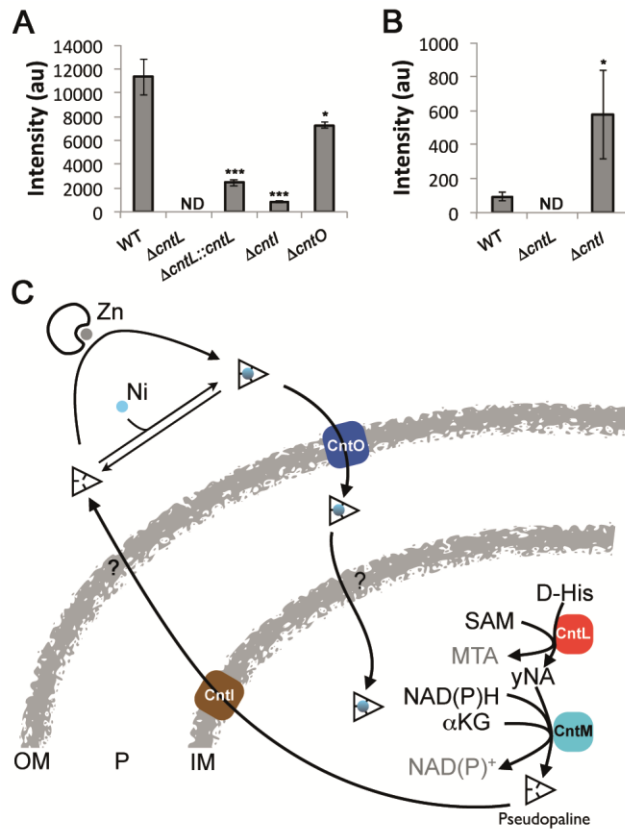414 pseudopaline from L-his, SAM, NADH and α-KG.

415
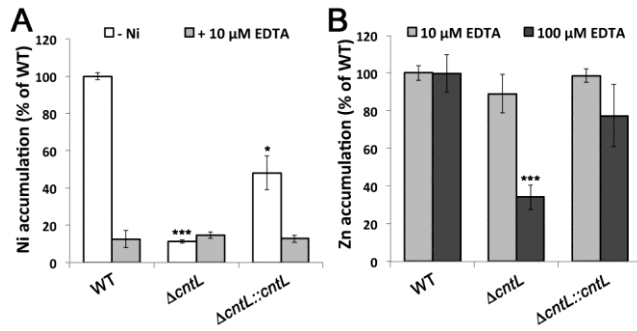
Figure 4: Pseudopaline is involved in nickel uptake in minimal media and in zinc uptake in chelating media. Intracellular nickel (A) or zinc (B) levels measured by ICP-MS in WT, *ΔcntL* and *ΔcntL::cntL* strains grown in MS medium supplemented or not with 10 or 100μM EDTA. Error bars, mean ± s.d. *$P<0.05$, **$P<0.01$ and ***$P<0.001$ as compared to the WT.

423

424   Figure 5: Model of pseudopaline synthesis, secretion and metal uptake in *P. aeruginosa.* (A)

425   Extracellular detection of pseudopaline in the extracellular fraction of WT and mutant strains.

426   Error bars, mean ± s.d. *$P<0.05$, ***$P<0.01$ and ****$P<0.001$ as compared to the WT. (B)

427   Intracellular detection of pseudopaline in the intracellular fraction of WT and mutant strains.

428   ND: Not Detectable. (C) Model of pseudopaline production, secretion and recovery of nickel

429   or zinc. Outer membrane (OM), inner membrane (IM), periplasm (P).

430

431